A New DNA Marker Tightly Linked to the Fragile X Locus (*FRAXA*)

G. K. SUTHERS,* D. F. CALLEN, V. J. HYLAND, H. M. KOZMAN, E. BAKER, H. EYRE, P. S. HARPER, S. H. ROBERTS, M. C. HORS-CAYLA, K. E. DAVIES, M. V. BELL, G. R. SUTHERLAND

The fragile X syndrome is the most common cause of familial mental retardation. Genetic counseling and gene isolation are hampered by a lack of DNA markers close to the disease locus. Two somatic cell hybrids that each contain a human X chromosome with a breakpoint close to the fragile X locus have been characterized. A new DNA marker (*DXS296*) lies between the chromosome breakpoints and is the closest marker to the fragile X locus yet reported. The Hunter syndrome gene, which causes iduronate sulfatase deficiency, is located at the X chromosome breakpoint that is distal to this new marker, thus localizing the Hunter gene distal to the fragile X locus.

THE LOCATIONS OF OVER 3500 genes, chromosomal fragile sites, and DNA segments have been mapped in the human genome (*1*). The localization of a gene in relation to nearby polymorphic DNA segments (or markers) allows for accurate carrier detection or prenatal diagnosis (*2*), and may be a critical step in the isolation of a particular disease gene (*3*). The fragile X syndrome is the most common cause of familial mental retardation and is associated with a chromosomal fragile site at Xq27.3 (*4*). The mutant locus (*FRAXA*) is located at or near the fragile site, but genetic counseling and gene isolation have been hampered by a lack of closely linked DNA markers (*5*) and the unusual genetics of the fragile X syndrome (*6*). The order of markers near *FRAXA* is cen–*F9*–*DXS105*–*DXS98*–*FRAXA*–*DXS374*–*DXS52*–qter (*5, 7*). These markers are widely used for carrier identification and prenatal diagnosis in families with the fragile X syndrome. However, the reliability of such genetic counseling is limited by the relatively large genetic distances between *FRAXA* and the closest flanking markers: *DXS374* lies approximately 18 centimorgans (cM) distal and *DXS98* lies approximately 5 cM proximal to *FRAXA* (*7, 8*).

In an attempt to isolate more DNA markers located near *FRAXA*, we generated a genomic library (*9*) from a somatic cell hybrid (CY3) containing the derived 16 of a t(X;16)(q26;q24) reciprocal translocation (*10*). This ensured that X-derived clones from the library were located in the region Xq26-qter. The translocation breakpoint in CY3 was between *HPRT* and *DXS100* (Table 1). We used two somatic cell hybrids, PeCHN and CY34, to physically map DNA clones from the library. PeCHN contained the derived X from a balanced t(X;21)(q27;q11) translocation (*11*), and the breakpoint was in the same interval as *FRAXA*, that is, *DXS98*–*DXS374* (Table 1). CY34 was derived from a girl with Hunter syndrome [iduronate sulfatase (IDS) deficiency; mucopolysaccharidosis II] and a t(X;5) reciprocal translocation. The translocation breakpoint was at Xq28, and the normal X chromosome was consistently inactivated (*12*). It was postulated that *IDS* was located at the breakpoint on the X chromosome. This localization was consistent with genetic linkage studies indicating that *IDS* lay between *F9* and *DXS52*. The translocated X chromosome was isolated in a hypoxanthine phosphoribosyltransferase (HPRT)–deficient mouse cell line as described (*10*).

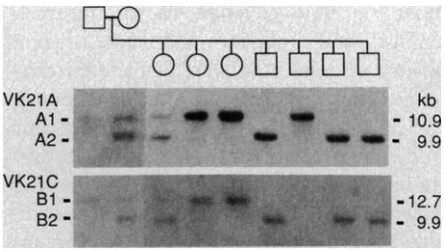

Fig. 1. Mendelian inheritance of the *DXS296* RFLPs. Probe VK21A is a 1.3-kb Hind III–Sal I fragment of VK21 cloned into the Hind III–Sal I sites of pBR328 (*21*); it detected a two-allele Taq I RFLP with a common allele (A1) frequency of 0.87 (111 chromosomes) among unrelated males and females from the CEPH pedigrees. VK21C is a 2.5-kb Hind III fragment of VK21 cloned into the Hind III site of pUC18; it detected a two-allele Msp I RFLP with a common allele (B1) frequency of 0.81 (116 chromosomes) in the CEPH pedigrees. Neither probe detected any constant bands. Among 35 unrelated CEPH males, 34 had A1B1 or A2B2 haplotypes and only one had an A1B2 haplotype, suggesting that a female homozygous for one RFLP would probably be homozygous for the other. Both probes were used to probe panels of genomic DNA (12 X chromosomes each) digested with the following enzymes: Taq I, Msp I, Rsa I, Hinc II, Sac I, Bgl II, Eco RI, Hind III, Pst I, and Pvu II; no other RFLPs were detected.

The translocation breakpoint in this hybrid cell line (CY34) was also between *DXS98* and *DXS374* (Table 1), indicating that *IDS* was in the same interval as *FRAXA*.

We isolated one clone (VK21) with a 16.7-kb insert that identified the marker *DXS296*. VK21 detected sequences on CY34 that were not present on PeCHN (Table 1). This indicated that the PeCHN breakpoint was proximal to the CY34 breakpoint and, as a corollary, that *DXS296* was proximal to *IDS*. Fragments of unique human DNA from the probe VK21 detected two restriction fragment length polymorphisms (RFLPs). A 1.3-kb fragment

Table 1. Xq-derived DNA markers used to define the breakpoints in somatic cell hybrid lines. DNA was extracted and digested with Hind III, as described (*16*). DNA probes (*7, 17*) were labeled with ^{32}P-dCTP (deoxycytidine triphosphate) and hybridized to Southern blots of the digested DNA. The presence (+) or absence (−) of the specified marker in each cell line is indicated. The cell line CY34 contained several human autosomes in addition to the derived X. CY34A is a subclone of CY34 and contained only a fragment of the derived X including the region Xq24–q27. CY34A arose spontaneously and was detected during routine cytogenetic screening of a series of subclones.

Region	Marker	Probe	Cell lines			
			CY3	PeCHN	CY34	CY34A
q21.33	*DXYS1*	pDP34	−	+	+	−
q21.33–q24	*DXS87*	A13.R1	−	+	+	−
q24–q25	*DXS42*	p43-15	−	+	+	+
q26	*DXS100*	pX45d	−	+	+	+
q26	*HPRT*	pHPT30	+	+	+	+
q27	*DXS105*	cX55.7	+	+	+	+
q27	*DXS98*	4D-8	+	+	+	+
q27–qter	*DXS374*	1A1	+	−	−	−
q28	*DXS52*	St14-1	+	−	−	−
	DXS296	VK21	+	−	+	+

G. K. Suthers, D. F. Callen, V. J. Hyland, H. M. Kozman, E. Baker, H. Eyre, G. R. Sutherland, Cytogenetics Unit, Department of Histopathology, The Adelaide Children's Hospital, North Adelaide SA 5006, Australia.
P. S. Harper and S. H. Roberts, Institute of Medical Genetics, University Hospital of Wales, Cardiff, United Kingdom.
M. C. Hors-Cayla, Unité de Recherches de Génétique Médicale, Hôpital des Enfants Malades, Paris, France.
K. E. Davies and M. V. Bell, Institute of Molecular Medicine, University of Oxford, Oxford, United Kingdom.

*To whom correspondence should be addressed.

Table 2. Two-point lod scores from pairwise analysis of *DXS296* and other loci in fragile X and CEPH pedigrees. The lod score is the logarithm (base 10) of the odds ratio in favor of linkage between the two loci at the specified recombination rate (*18*). The peak lod score ($\hat{z}$) indicates the most likely recombination rate ($\hat{\theta}$) in the pedigrees analyzed. Linkage analysis in the fragile X pedigrees was performed with genotype data from seven multigeneration pedigrees with more than one affected individual. The *FRAXA* locus frequency and penetrance classes were as described (*16*); the *FRAXA* mutation rate (0.00024) was assumed to be equal in males and females (*19*). For analysis in the CEPH pedigrees, published genotypes from the CEPH database, version 2, were used. Linkage analyses were performed with the LINKAGE package, version 4.7 (*20*). The number of families informative at both loci (n) ranged from 2 to 7. The results from analysis in the CEPH pedigrees are shown in parentheses under the results from analysis in the fragile X pedigrees; ND, no data.

DXS296 in relation to	Recombination fractions							$\hat{z}$	$\hat{\theta}$	n
	0.001	0.01	0.05	0.10	0.20	0.30	0.40			
F9	−11.88	−5.97	−2.00	−0.93	−0.24	−0.19	−0.18	0.00	0.50	5
	(−6.89)	(−2.95)	(−0.42)	(0.43)	(0.87)	(0.72)	(0.33)	(0.88)	(0.21)	(3)
DXS105	1.13	1.11	1.04	0.95	0.76	0.54	0.29	1.13	0.00	2
	(−2.09)	(−0.14)	(1.04)	(1.36)	(1.35)	(1.02)	(0.53)	(1.42)	(0.14)	(2)
DXS98	1.25	1.22	1.10	0.93	0.57	0.19	−0.06	1.25	0.00	6
	(−1.50)	(−0.52)	(0.93)	(0.28)	(0.32)	(0.22)	(0.08)	(0.33)	(0.17)	(1)
FRAXA	6.24	6.13	5.62	4.96	3.56	2.11	0.85	6.25	0.00	7
	(ND)	(ND)	(ND)	(ND)	(ND)	(ND)	(ND)	(ND)	(ND)	(0)
DXS374	ND	ND	ND	ND	ND	ND	ND	ND	ND	0
	(−2.69)	(−0.74)	(0.46)	(0.81)	(0.85)	(0.74)	(0.21)	(0.89)	(0.16)	(3)
DXS52	−6.23	−1.33	1.68	2.52	2.48	1.60	0.52	2.66	0.14	7
	(−13.76)	(−3.95)	(2.22)	(4.15)	(4.81)	(3.92)	(2.20)	(4.87)	(0.18)	(7)

(VK21A) detected a Taq I RFLP, and a 2.5-kb fragment (VK21C) detected an Msp I RFLP (Fig. 1). Linkage analysis of *DXS296* in relation to *F9, DXS105, DXS98, DXS374*, and *DXS52* was carried out in 27 normal pedigrees from the Centre d'Etude du Polymorphisme Humain (CEPH) (Table 2). The order *F9–DXS105–DXS98–DXS374–DXS52* was assumed, and the likelihood of *DXS296* being located in each interval was assessed. The most likely order (by a factor of 40) was *F9–DXS105–DXS98–DXS296–DXS374–DXS52*. Further multipoint linkage analysis in the CEPH pedigrees was not performed as the CEPH X-chromosome consortium map has yet to be published. Multipoint linkage analysis of *DXS296* in relation to *F9, DXS98, FRAXA*, and *DXS52* was performed in seven fragile X pedigrees. The order *F9–DXS98–FRAXA–DXS52* and the following recombination fractions were assumed: *FRAXA–F9* (0.20), *FRAXA–DXS98* (0.05), and *FRAXA–DXS52* (0.15) (*5, 8*). Haldane's mapping function was used; other details of the genetic model are given in the legend of Table 2. The most likely location of *DXS296* was within 1 cM of *FRAXA*. Two-point linkage analysis (Table 2) indicated that there was no recombination between *DXS296* and *FRAXA* with the peak lod score of 6.25 at a recombination rate of zero. The approximate 90% confidence interval (*13*) for the recombination rate between *DXS296* and *FRAXA* was 0.00 to 0.08.

The physical location of *DXS296* in relation to the fragile site at Xq27.3 was examined by in situ hybridization (*14*) of the probe VK21A. Of the 139 silver grains that touched the X chromosome and could be scored relative to the fragile site, 70 grains were distal and lay between the fragile site and the telomere, 43 grains lay within a similar distance proximal to the fragile site, and 26 grains were located centrally over the chromosome gap at the fragile site. The difference between the number of proximal versus distal grains was significant ($\chi^2 = 6.45$, $P < 0.02$), indicating that *DXS296* was distal to the fragile site.

The order of loci at Xq27–28 is therefore cen–*F9–DXS105–DXS98–FRAXA–DXS296–IDS–DXS374–DXS52*–qter. Two other DNA markers have recently been isolated in this region (*15*). *DXS369* is probably in the interval *DXS98–FRAXA* at a distance of 5 cM from *FRAXA*. *DXS304* is 3 cM from *FRAXA* and lies distal to the CY34 breakpoint in the interval *IDS–DXS374*. In contrast to these two markers, the new marker *DXS296* is tightly linked to *FRAXA* and is the closest published marker to that locus. The availability of the probe VK21 for the genetic counseling of families with the fragile X syndrome will reduce the diagnostic uncertainty inherent in using more distant markers. Furthermore, *DXS296* and *DXS304* closely flank *IDS* and will be valuable in genetic counseling of families with an established mutation at *IDS* that causes Hunter syndrome. The frequency of females heterozygous for the *DXS296* RFLPs (Fig. 1) limits the number of families in which VK21 will be useful for genetic counseling, but this will not restrict its usefulness in the development of large-scale restriction maps around *FRAXA* and *IDS*. The translocation breakpoint in the somatic cell hybrid PeCHN lies in the interval *DXS98–DXS296*. The translocation breakpoint in the cell line CY34 is at *IDS* and is distal to *FRAXA*. These two cell lines will allow for the rapid identification of more DNA markers that are physically close to *FRAXA* and *IDS*.

REFERENCES AND NOTES

1. P. J. McAlpine *et al.*, *Cytogenet. Cell Genet.* **49**, 4 (1988).
2. J. F. Gusella, *Annu. Rev. Biochem.* **55**, 831 (1986).
3. A. P. Monaco and L. M. Kunkel, *Trends Genet.* **3**, 33 (1987).
4. G. R. Sutherland and F. Hecht, *Fragile Sites on Human Chromosomes* (Oxford Univ. Press, New York, 1985).
5. K. E. Davies, J.-L. Mandel, J. Weissenbach, M. Fellous, *Cytogenet. Cell Genet.* **46**, 277 (1987).
6. S. L. Sherman *et al.*, *Hum. Genet.* **69**, 289 (1985).
7. M. N. Patterson *et al.*, *Genomics* **4**, 570 (1989).
8. R. E. Schnur *et al.*, *Am. J. Hum. Genet.* **44**, 248 (1989).
9. V. J. Hyland *et al.*, *Hum. Genet.* **83**, 61 (1989).
10. D. F. Callen, *Ann. Genet.* **4**, 235 (1986).
11. J. Couturier *et al.*, *Hum. Genet.* **49**, 319 (1979).
12. J. Mossman, S. Blunt, R. Stephens, E. E. Jones, M. Pembrey, *Arch. Dis. Child.* **58**, 911 (1983); S. H. Roberts, M. Upadhyaya, M. Sarfarazi, P. S. Harper, *J. Med. Genet.* **26**, 309 (1989).
13. P. M. Conneally *et al.*, *Cytogenet. Cell Genet.* **40**, 356 (1985).
14. R. N. Simmers *et al.*, *Hum. Genet.* **78**, 134 (1988).
15. J.-L. Mandel *et al.*, *Cytogenet. Cell Genet.* **51**, 384 (1989).
16. J. C. Mulley, A. K. Gedeon, K. A. Thorn, L. J. Bates, G. R. Sutherland, *Am. J. Med. Genet.* **27**, 435 (1987).
17. P. L. Pearson, K. K. Kidd, H. F. Willard, *Cytogenet. Cell Genet.* **46**, 390 (1987).
18. J. Ott, *Analysis of Human Genetic Linkage* (Johns Hopkins Univ. Press, Baltimore, MD, 1985).
19. S. L. Sherman, A. Rogatko, G. Turner, *Am. J. Med. Genet.* **31**, 753 (1988).
20. G. M. Lathrop, J. M. Lalouel, C. Julier, J. Ott, *Am. J. Hum. Genet.* **37**, 482 (1985).
21. S. L. Berger and A. R. Kimmel, Eds., *Guide to Molecular Cloning Techniques* (Academic Press, Orlando, FL, 1987).

22. Supported by the Australian National Health and Medical Research Council and The Adelaide Chil-

dren's Hospital Research Foundation. The Centre d'Etude du Polymorphisme Humain provided DNA samples and computer software. The cell lines described in this paper and the DNA probe VK21 (including VK21A and VK21C) are available on a collaborative basis.

11 July 1989; accepted 6 October 1989

Cell Cycle–Dependent Regulation of Phosphorylation of the Human Retinoblastoma Gene Product

KOICHIRO MIHARA, XIANG-RONG CAO, ANDREW YEN, SUZANNE CHANDLER, BARBARA DRISCOLL, A. LINN MURPHREE, ANNE T'ANG, YUEN-KAI T. FUNG*

The human retinoblastoma gene (*RB1*) encodes a protein (Rb) of 105 kilodaltons that can be phosphorylated. Analysis of Rb metabolism has shown that the protein has a half-life of more than 10 hours and is synthesized at all phases of the cell cycle. Newly synthesized Rb is not extensively phosphorylated (it is "underphosphorylated") in cells in the G_0 and G_1 phases but is phosphorylated at multiple sites at the G_1/S boundary and in S phase. HL-60 cells that were induced to terminally differentiate by various chemicals lost their ability to phosphorylate newly synthesized Rb at multiple sites when cell growth was arrested. These findings suggest that underphosphorylated Rb may restrict cell proliferation.

WHEN ACTIVELY PROLIFERATING cells are deprived of growth factors, they become arrested at the G_0 phase of the cell cycle. Conversely, quiescent cells are induced to proliferate when provided with the appropriate growth factors. Exposure of quiescent cells to growth stimuli leads to quantitative and qualitative changes in the expression of many specific genes and their products. For example, exposure of resting cells to platelet-derived growth factor (PDGF) (*1*) or epidermal growth factor (EGF) (*2*) leads to the activation of the respective receptor tyrosine kinases, which may then directly phosphorylate phospholipase C. This, in turn, may result in other biochemical responses such as the hydrolysis of phosphoinositides, the elevation of intracellular Ca^{2+}, the modulation of protein phosphorylation, and the induction of synthesis of new mRNA [reviewed in (*3*)]. Because some of the transcriptionally activated genes are proto-oncogenes, studies on the control of cell proliferation have mainly focused on the isolation and characterization of similar genes, the expression of which is activated in the early hours of the proliferative response (*4*). A number of genes that are expressed specifically in the quiescent state have also been isolated (*5*). The expression of these genes is repressed when a cell is exposed to growth stimuli. Therefore, downregulation of specific genes may also be important for the mitogenic response, by removing blocks to cell proliferation.

The human retinoblastoma gene, *RB1*, is the prototype of a class of genes in which the inactivation of both alleles is thought to be essential for neoplastic growth. The isolation of *RB1* has allowed a confirmation at the molecular level of the loss of the gene in retinoblastoma and clinically related tumors, such as osteosarcomas (*6*). Moreover, analyses using the *RB1* cDNA probe and antibodies to its gene product (Rb) have revealed the loss of *RB1* in a large number of tumors seen in adults, such as small cell lung carcinoma (*7*) and breast tumors (*8*). That *RB1* may have an important function in the control of neoplastic growth is supported by the fact that Rb forms a physical association with the transformation proteins of several viruses: E1A of adenovirus (*9*), large T antigen of simian virus 40 (SV40) (*10*), and the E7 protein of human papillomavirus type 16 (*11*). As the inactivation of *RB1* is associated with tumorigenesis, it is possible that the function of Rb is to restrict cell proliferation. We have examined the regulation of Rb expression in cells under various growth conditions.

Peptides representing the most hydrophilic regions of Rb were synthesized and used to immunize rabbits and BALB/c mice for the production of polyclonal and monoclonal antibodies (*12*). Multiple forms of Rb, with apparent molecular masses from 105 to 115 kD, could be detected by immunoprecipitation from the human bladder tumor cell line VM-CUB-3 labeled with [^{35}S]methionine, followed by SDS–polyacrylamide gel electrophoresis (SDS-PAGE) (Fig. 1A, lane 1). No such protein could be precipitated when the antibodies were preabsorbed with the corresponding Rb peptides (Fig. 1A, lane 2). Metabolic labeling with [^{32}P]orthophosphate demonstrated that the Rb polypeptides with higher apparent molecular mass were more heavily phosphorylated (Fig. 1A, lane 3). Treatment of the phosphoproteins with potato acid phosphatase before immunoprecipitation resulted in the disappearance of these Rb species (*13*). Immunohistochemical staining of cells with these antibodies revealed the nuclear localization of Rb as has been described (*14*) and is predicted from the presence of a sequence of amino acids, VRSPKKK (residues 609 to 615) (*15*), reminiscent of the nuclear translocation signal found in SV40 large T antigen.

To determine whether the synthesis and degradation of Rb is regulated in a cell cycle–dependent manner, we measured the steady-state amount of Rb as a function of the cell cycle. Because the rabbit polyclonal antibodies Rb 1-AB 20, Rb 1-AB 16, and Rb 1-AB A1 detect the various phosphorylated forms of Rb, it was possible to measure the total amount of Rb in cells. Exponentially proliferating wild-type HL-60 cells were fixed and stained with Rb 1-AB 20 and a secondary fluorescein-conjugated antibody to rabbit immunoglobulin G (IgG). The cells were then treated with ribonuclease A (RNase A), and stained with propidium iodide for quantitation of DNA. Because fluorescein emission is green and propidium iodide emission is red, when the cells are irradiated at 488 nm, it is possible to simultaneously measure the emission intensities, and therefore the Rb and DNA content, by flow cytometry (Fig. 1B). The amount of Rb per cell increased as the cells progressively matured through the G_1, S, and G_2 + M phases of the cell cycle. Cells in the G_2 + M phases contain approximately twice as much Rb as cells entering G_1. Therefore, the Rb content of a proliferating cell is always maintained at or above the threshold level in G_0 and G_1. This would be expected if the rate of Rb synthesis exceeds that of its degradation. These results were reproduced when the experiments were performed with Rb 1-AB A1 (*13*).

To understand the dynamics of Rb turnover, we studied the synthesis and degradation of Rb with immunoprecipitation techniques. The human breast tumor cell line SW613 was pulse-labeled for 90 min with [^{35}S]methionine, and the degradation rate of labeled Rb was monitored (Fig. 1C).

K. Mihara, X.-R. Cao, B. Driscoll, A. L. Murphree, A. T'Ang, Y.-K. T. Fung, Division of Hematology/Oncology and Ophthalmology, Childrens Hospital of Los Angeles, and Departments of Pediatrics, Ophthalmology, and Microbiology, School of Medicine, University of Southern California, Los Angeles, CA 90027.
A. Yen and S. Chandler, Department of Pathology, College of Veterinary Medicine, Cornell University, Ithaca, NY 14853.

*To whom correspondence should be addressed.